International Journal of Nanomedicine

Dovepress
open access to scientific and medical research

Open Access Full Text Article

ORIGINAL RESEARCH

Porous Se@SiO_2 nanospheres attenuate ischemia/reperfusion (I/R)-induced acute kidney injury (AKI) and inflammation by antioxidative stress

This article was published in the following Dove Medical Press journal:
International Journal of Nanomedicine

Zhihuang Zheng[1,*]
Guoying Deng[2,*]
Chenyang Qi[3]
Yuyin Xu[3]
Xijian Liu[4]
Zhonghua Zhao[3]
Zhigang Zhang[3]
Yuening Chu[1]
Huijuan Wu[3]
Jun Liu[1]

[1]Department of Nephrology, Shanghai General Hospital, Shanghai Jiao Tong University School of Medicine, Shanghai, China; [2]Trauma Center, Shanghai General Hospital, Shanghai Jiao Tong University School of Medicine, Shanghai, China; [3]Department of Pathology, School of Basic Medical Sciences, Fudan University, Shanghai, China; [4]Department of Chemical Engineering and Technology, College of Chemistry and Chemical Engineering, Shanghai University of Engineering Science, Shanghai, China

*These authors contributed equally to this work

Correspondence: Huijuan Wu
Department of Pathology, School of Basic Medical Sciences, Fudan University, 131 Dongan Road, Shanghai 200032, China
Tel +86 54237528-2041
Fax +86 21 5423 7596
Email hjwu@shmu.edu.cn

Jun Liu
Department of Nephrology, Shanghai General Hospital, Shanghai Jiao Tong University School of Medicine, 650 Xinsongjiang Road, Shanghai 201620, China
Tel +86 6324 0090 8961
Fax +86 21 6324 0825
Email liujun-sgh@sjtu.edu.cn

Objectives: Acute kidney injury (AKI) is a growing global health concern, and is associated with high rates of mortality and morbidity in intensive care units. Se is a trace element with antioxidant properties. This study aimed to determine whether porous Se@SiO_2 nanospheres could relieve oxidative stress and inflammation in ischemia/reperfusion (I/R)-induced AKI.

Methods: Male 6- to 8-week-old C57bl/6 mice were divided into four groups: sham + saline, sham + Se@SiO_2, I/R + saline, and I/R + Se@SiO_2. Mice in the I/R groups experienced 30 minutes of bilateral renal I/R to induce an AKI. Porous Se@SiO_2 nanospheres (1 mg/kg) were intraperitoneally injected into mice in the I/R + Se@SiO_2 group 2 hours before I/R, and the same dose was injected every 12 hours thereafter. Hypoxia/reoxygenation (H/R) was used to mimic I/R in vitro. PBS was used as a control treatment. Human kidney 2 cells were seeded into 12-well plates (5×10^5 cells/well) and divided into four groups: control + PBS group, control + Se@SiO_2 group, H/R + PBS group, and H/R + Se@SiO_2 group (n=3 wells). We then determined the expression levels of ROS, glutathione, inflammatory cytokines and proteins, fibrosis proteins, and carried out histological analysis upon kidney tissues.

Results: In vitro, intervention with porous Se@SiO_2 nanospheres significantly reduced levels of ROS ($P<0.05$), inflammatory cytokines ($P<0.05$), and inflammation-associated proteins ($P<0.05$). In vivo, tubular damage, cell apoptosis, and interstitial inflammation during AKI were reduced significantly following treatment with porous Se@SiO_2 nanospheres. Moreover, the occurrence of fibrosis and tubular atrophy after AKI was attenuated by porous Se@SiO_2 nanospheres.

Conclusion: Porous Se@SiO_2 nanospheres exhibited a protective effect in I/R-induced AKI by resisting oxidative stress and inflammation. This suggests that porous Se@SiO_2 nanospheres may represent a new therapeutic method for AKI.

Keywords: acute kidney injury, ischemia/reperfusion, porous Se@SiO_2 nanospheres, oxidative stress, inflammation

Introduction

Acute kidney injury (AKI) is estimated to occur in 20–200 patients per million of the global population; 7%–18% of these patients remain in hospital and ~50% of patients are admitted to intensive care units (ICUs).[1–3] Furthermore, AKI has been widely recognized as being an important risk factor which can lead to the occurrence and progression of chronic kidney disease (CKD).[4–6] Ischemic injury is the main cause of AKI, although at present, there is a significant lack of therapeutic options for treatment.[7] However, research has provided strong evidence that oxidative stress and inflammation are major contributors to the pathogenesis of ischemic AKI.[8–11] Ischemia/reperfusion (I/R)

submit your manuscript | www.dovepress.com
Dovepress
http://dx.doi.org/10.2147/IJN.S184804

injury can lead to the production of large amounts of reactive oxygen species (ROS) in tubular epithelial cells (TECs), thus triggering mitochondrial damage and lipid peroxidation and causing devastating cell damage. The inflammatory factors produced by TECs cause a large number of inflammatory cells to migrate and infiltrate, further aggravating renal damage, and subsequently, inflammation amplification.[12–14]

Recent studies have provided evidence that TEC-associated inflammation aggravates kidney injury and impairs tissue repair after I/R injury.[15] It has also been demonstrated that nuclear factor-κB (NF-κB) and NACHT, LRR, and PYD domains-containing protein 3 (NLRP3) are involved in mediating injury and inflammation associated with ischemic AKI.[16–18] Activation of NF-κB, and the accumulation of NLRP3, can cause levels of the effector molecule caspase-1 to increase, which can then promote the production of interleukin-1β (IL-1β), thus amplifying inflammation and aggravating damage. Therefore, it is particularly important to explore the early damage mechanisms underlying AKI and to intervene and treat this condition, particularly if we wish to prevent the transition from AKI to CKD.

Se is a natural trace element and an ingredient of glutathione peroxidase. Porous Se@SiO_2 nanospheres are a new material synthesized by the use of nanotechnology. These nanospheres can directly or indirectly scavenge intracellular free radicals and ROS, thus inhibiting oxidative stress.[19] Our previous studies showed that porous Se@SiO_2 nanospheres can effectively relieve acute stress damage in the mice heart, and rats' femoral head and lungs.[20–22] However, this has not yet been investigated for potential applications in kidney disease. Therefore, we hypothesized that porous Se@SiO_2 nanospheres may have therapeutic significance for I/R-induced AKI. To test this hypothesis, we studied the pattern and dynamics of ROS production, and the expression of inflammation-associated proteins in severe AKI models induced by I/R injury.

Materials and methods

Synthesis and characterization of porous Se@SiO_2 nanospheres

Porous Se@SiO_2 nanospheres (College of Chemistry and Chemical Engineering, Shanghai University of Engineering Science, Shanghai, China) used herein were synthesized as described in our previous study.[21,23] Firstly, $Cu_{2-x}Se$ nanocrystals were prepared and mixed with n-hexanol, n-hexane, deionized water, Triton X-100, and tetraethyl orthosilicate. $[Cu(NH_3)_4]^{2+}$ was developed by adding ammonium hydroxide to the mixture. Oxygen was used to oxidize Se^{2-} to develop Se quantum dots. In an alkaline environment, the silica was coated upon the Se quantum dots by orthosilicate hydrolysis, thus forming solid Se@SiO_2 nanospheres. Then, the solid Se@SiO_2 nanospheres were coated with polyvinylpyrrolidone. After treatment with hot water, the Se@SiO_2 nanospheres formed porous structures. Porous Se@SiO_2 nanospheres were characterized by means of a D/max-2550 PC X-ray diffractometer (XRD; Rigaku Corporation, Tokyo, Japan; Cu-Kα radiation) and transmission electron microscopy (TEM; JEM-2100F; JEOL, Tokyo, Japan). Synthesized porous Se@SiO_2 nanospheres were then dispersed in deionized water for subsequent experiments.

Animal experiments

Male gender confers a greater susceptibility to I/R renal injury and avoids the interference of estrogen in experimental results.[24–27] Thus, our experiments involved 6- to 8-week-old male C57bl/6 mice, weighing 20–22 g (SLAC Laboratory Animal Center, Shanghai, China). In total, 60 mice were randomly divided equally (n=15) into four groups: sham + saline, sham + Se@SiO_2, I/R + saline, and I/R + Se@SiO_2 (Table 1). The I/R group mice were exposed to 30 minutes of bilateral renal I/R to induce an AKI. In the I/R + Se@SiO_2 group, 1 mg/kg of porous Se@SiO_2 nanospheres was intraperitoneally injected 2 hours before I/R, and the same

Table 1 Treatments and survivals of different experimental mice groups

Treatment groups (n=15)	Three subgroups (n=5)		
	24 hours after operation survival (operated mice)	72 hours after operation survival (operated mice)	2 weeks after operation survival (operated mice)
Sham + saline	5	5	5
Sham + Se@SiO_2	5	5	5
I/R + saline	4	4	4
I/R + Se@SiO_2	5	4	5

Notes: Mice were randomly divided equally (n=15) into sham + saline group, sham + Se@SiO_2 group, I/R + saline group, and I/R + Se@SiO_2 group. Each group was further subdivided into three time point subgroups at 24 hours, 72 hours, 2 weeks (n=5), respectively. Mice (n=56) that survived after I/R or sham operation challenge were to receive either saline or Se@SiO_2 (1 mg/kg/12 h).
Abbreviations: I/R, ischemia/reperfusion; sham, sham operation without I/R.

dose of porous Se@SiO_2 nanospheres was injected every 12 hours thereafter. The sham groups were injected with the same amount of saline and Se@SiO_2, respectively. Each group was randomly divided into three subgroups (Table 1), which were sacrificed at 24 hours, 72 hours, and 2 weeks after the initial surgery. Serum samples were then collected and stored at −80°C for detection and analysis. Both kidneys were immediately removed from the culled animals and processed for histological evaluation and protein extraction. The animal experimental protocol used herein was in accordance with the guidelines of the National Institutes of Health Guide for the Care and Use of Laboratory Animals and was approved by the Ethics Committee of Shanghai General Hospital.

Renal function

In order to evaluate renal function, we measured blood urea nitrogen (BUN) and creatinine (Cr) levels in the serum using commercial kits (Jiancheng Bioengineering Institute, Nanjing, China).

ELISA

ELISA kits, including mouse IL-1β, monocyte chemotactic protein-1 (MCP-1), tumor necrosis factor-α (TNF-α), and human glutathione (GSH), were purchased from Jiancheng Bioengineering Institute. Cell culture supernatants were collected and centrifuged for 10 minutes at a speed of 1,500 rpm. Levels of cytokines and GSH in the cell supernatant were subsequently determined according to the relevant manufacturer's protocol. All test indicators were performed in triplicate.

Histology and apoptosis evaluation

Renal histology was subjected to a blind examination after H&E staining. Severe injury, restricted to the highly susceptible outer medullary regions, is known to result in significant tubular damage and atrophy over the long term.[15,28] Tissue damage was then scored according to the proportion (%) of damaged tubules: 0, no damage; 1, <25% damage; 2, 25%–50% damage; 3, 50%–75% damage; and 4, >75% damage.[29] The criteria for tubular damage included the loss of brush border, tubular dilation, cast formation, and cell lysis. For quantification, 10 fields per section were randomly selected at a magnification of ×200 for evaluation and scoring. Tubular atrophy was also scored in the same way: 0, no atrophy; 1, <25% atrophy; 2, 25%–50% atrophy; 3, 50%–75% atrophy; and 4, >75% atrophy. Ten fields per section were randomly selected at a magnification of ×200 for evaluation and scoring. The TUNEL assay was also carried out according to the manufacturer's protocol (In Situ Cell Death Detection Kit, POD; Hoffman-La Roche Ltd, Basel, Switzerland). Ten fields per section were randomly selected from each tissue section at a magnification of ×200 for evaluation.

Renal immunohistochemistry

The kidneys were removed and fixed in 4% paraformaldehyde, embedded in paraffin, and cut into 3-μm sections. Sirius Red, Masson's trichrome, and monoclonal mouse anti-α-smooth muscle actin (α-SMA; 1:200 dilution; Cell Signaling Technology, Danvers, MA, USA) stains were used to estimate fibrosis. Immunohistochemistry was performed to assess renal tubular injury and macrophage infiltration. For immunohistochemistry, kidney tissues sections were first deparaffinized and then incubated with 0.1 M sodium citrate (pH 6.0) at 98°C for antigen retrieval for 15 minutes. After incubation with blocking buffers, tissue sections were exposed sequentially to the primary antibody, and then a biotinylated secondary antibody (Dako REAL™ EnVision™; Dako Denmark A/S, Glostrup, Denmark). Immunohistochemical positive staining was consecutively revealed by the 3,3′-Diaminobenzidine Peroxidase Substrate Kit (Dako REAL™ EnVision™; Dako Denmark A/S) in accordance with the manufacturer's instructions. The following antibodies were used: monoclonal rabbit anti-neutrophil gelatinase-associated lipocalin (NGAL; 1:200 dilution; Abcam, Cambridge, UK) and monoclonal rabbit anti-F4/80 (1:200 dilution; Cell Signaling Technology). We randomly chose 10 fields at ×200 magnification in each slide to score the severity of interstitial fibrosis (Masson, Sirius Red, and α-SMA staining): 0, no evidence of interstitial fibrosis; 1, <10% involvement; 2, 10% to <25% involvement; 3, 25% to <50% involvement; and 4, 50% to <75% involvement; and 5, >75% involvement. NGAL staining was then scored according to the proportion (%) of positive areas: 0, no positive; 1, <10% positive; 2, 10%–20% positive; 3, 20%–30% positive; 4, 30%–40% positive; and 5, >40% positive. For quantification, 10 fields per section were randomly selected at a magnification of ×200 for evaluation and scoring.

Cell culture and hypoxia/reoxygenation (H/R)

Human kidney 2 (HK-2; FuHeng Cell Center, Shanghai, China) cells, a proximal tubular cell line derived from normal kidneys, were grown in DMEM/nutrient mixture F-12 (DMEM/F-12; HyClone Laboratories Inc, Logan, UT, USA) with 10% FBS (Thermo Fisher Scientific, Waltham, MA, USA), 100 μg/mL streptomycin, and 100 U/mL peni-

cillin (Thermo Fisher Scientific). The cells were cultured at 37°C in a 5% CO_2 incubator, and the culture medium was changed every 2–3 days. The cells were digested with 0.25% trypsin (Thermo Fisher Scientific) and passaged when they reached 80%–90% confluency. The cells were then exposed to an anaerobic medium (serum- and glucose-free) in a hypoxia incubator chamber (STEMCELL Technologies, Vancouver, BC, Canada) with an anoxic mixture gas (95% N_2 and 5% CO_2) for 12 hours at 37°C followed by reoxygenation for 1.5 hours with fresh culture medium (95% air and 5% CO_2) to simulate I/R injury.

Cell viability assays

The influence of porous Se@SiO_2 nanospheres on cell viability was detected with a cell counting kit-8 (CCK-8; Yeasen Biological Technology, Shanghai, China). HK-2 cells (8×10^3/well) were grown and treated with porous Se@SiO_2 nanospheres for 24 hours in 96-well plates. The concentrations of porous Se@SiO_2 nanospheres applied to HK-2 cells were 0, 10, 20, 40, 80, 100, 150, 200, 400, and 600 μg/mL. After 24 hours, 10 μL of CCK-8 solution was added to each well, and the plates were incubated for 2 hours. The absorbance at 450 nm was then measured using a multimode reader (Multiskan GO; Thermo Fisher Scientific).

Assay for intracellular ROS production

H/R was used to mimic I/R in vitro with PBS as a control treatment. HK-2 cells were seeded into 12-well plates (5×10^5 cells/well) and divided into four groups: control + PBS group, control + Se@SiO_2 group, H/R + PBS group, and H/R + Se@SiO_2 group (n=3 wells). The H/R + Se@SiO_2 group was pre-stimulated using porous Se@SiO_2 nanospheres at a final concentration of 40 μg/mL for 6 hours. H/R groups were exposed to H/R. The levels of intracellular ROS were subsequently detected with a ROS assay kit (Jiancheng Bioengineering Institute). Fluorescent signals were then determined with a fluorescence microscope (Zeiss LSM 800; Carl Zeiss Meditec AG, Jena, Germany). The production of ROS was quantified by using ImageJ software (National Institutes of Health, Bethesda, MD, USA). ROS ratio (%) = (each group mean OD value/normal control (NC) + PBS group mean OD value) ×100%. For quantification, 10 fields from each group were randomly selected at a magnification of ×400. In the assessment of all fields, identical analysis settings and thresholds were employed.

Western blotting

HK-2 cells were cultured in six-well plates. Two wells were treated as one treatment group and divided into three groups (n=2 wells): control + PBS group, H/R + PBS group, and H/R + Se@SiO_2 group. HK-2 cells and renal tissue from the outer medulla area were lysed and denatured at 100°C for 5 minutes in SDS buffer and separated by 10% PAGE. Proteins were then transferred onto 0.45-μm polyvinylidene difluoride membranes (EMD Millipore, Billerica, MA, USA), blocked for 1 hour with 5% dried nonfat skimmed milk powder in TBS-Tween-20 (TBS containing 0.1% Tween 20), and probed with appropriate antibodies. The following primary antibodies were used: monoclonal rabbit antibodies anti-phospho-NF-κB (1:1,000 dilution; Cell Signaling Technology), anti-NLRP3 (1:1,000 dilution; Cell Signaling Technology), anti-collagen type I, anti-collagen type III (1:1,000 dilution; Abcam), anti-NGAL (1:1,000 dilution; Abcam), and caspase-1 (1:1,000 dilution; Proteintech, Wuhan, China) and monoclonal rabbit antibodies anti-glyceraldehyde-3-phosphate dehydrogenase and anti-β-actin (1:2,000 dilution; Proteintech). Positive protein binding was visualized by a horseradish peroxidase-conjugated secondary antibody followed by the use of an enhanced chemiluminescence kit (New Cell Molecular Biotech, Suzhou, China).

Statistical analysis

Qualitative data, including histological tissue images, were representative of at least three experiments. Quantitative data were expressed as means ± SD. Statistical analysis was conducted using GraphPad Prism 5 (Graphpad Software Inc, La Jolla, CA, USA). Multiple groups were compared by ANOVA followed by Tukey's posttests. Statistical differences between two groups were determined by two-tailed unpaired or paired *t*-tests. $P<0.05$ was considered to be significantly different.

Results

Structure, characterization, and toxicity of porous Se@SiO_2 nanospheres

Porous Se@SiO_2 nanospheres were prepared according to a previous methodology.[23] The phase structure of the porous Se@SiO_2 nanospheres was detected by an XRD pattern (Figure 1Aa). There were several well-defined characteristic peaks, such as (100), (011), (110), and (012), indicating the hexagonal phase and referenced as the standard Se phase (Joint Committee on Powder Diffraction Standards card no 65-1876). In addition, due to the amorphous silica coating, the XRD pattern of porous Se@SiO_2 nanospheres showed a steady increase in the low angle region. TEM (Figure 1Ab) showed that the porous Se@SiO_2 nanospheres had a diameter of ~55 nm, and that many very small nanoparticles

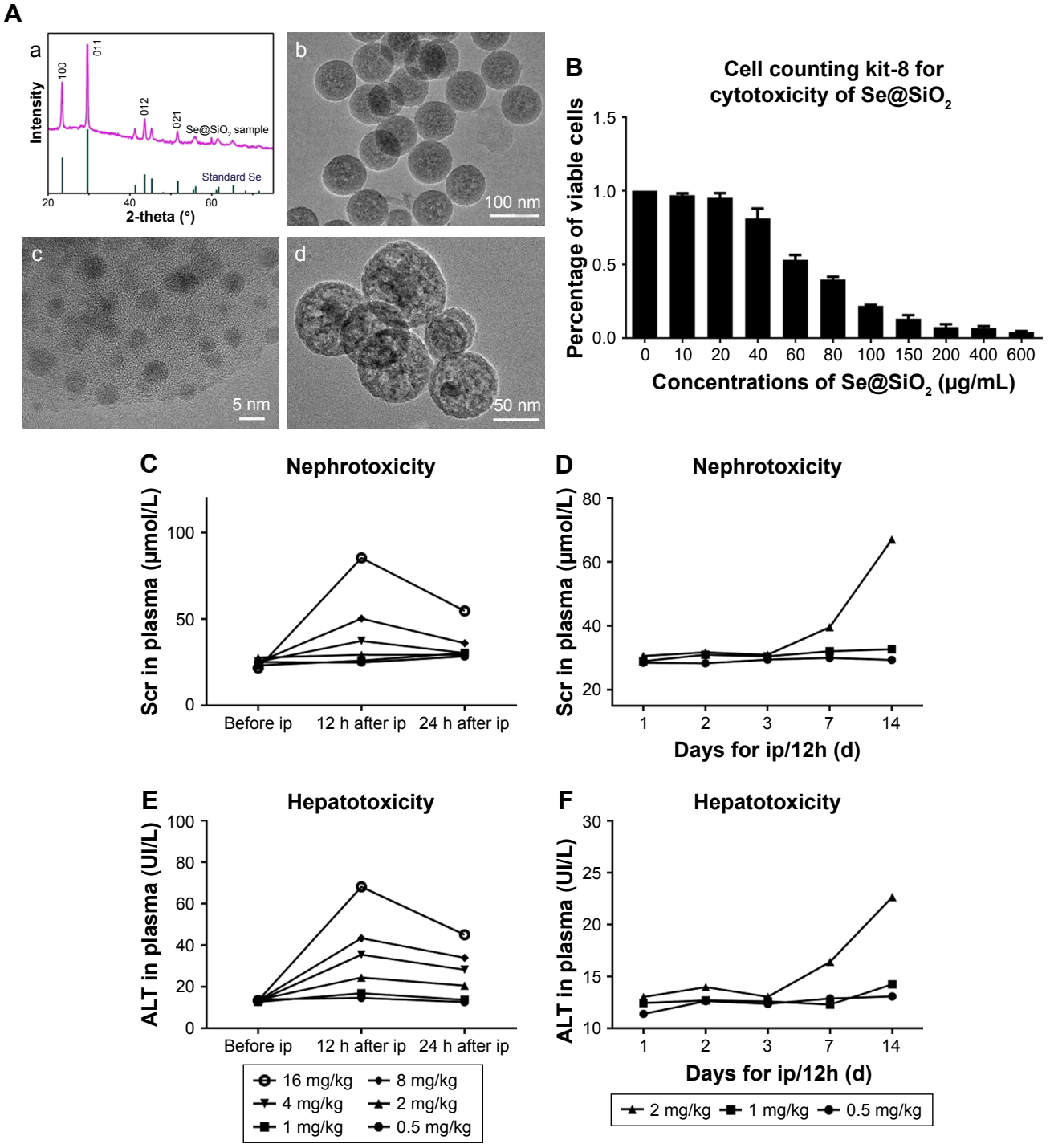

Figure 1 Structure, characterization, and toxicity of porous Se@SiO_2 nanocomposites.

Notes: (**A**) Characterization of porous Se@SiO_2 nanospheres: (a) XRD pattern of the porous Se@SiO_2 nanospheres and standard hexagonal phase of Se (Joint Committee on Powder Diffraction Standards and no 65-1876). (b) TEM of porous Se@SiO_2 nanospheres. (c) Low magnification and (d) high magnification images of porous Se@SiO_2 nanospheres. (**B**) The influence of porous Se@SiO_2 nanospheres on the viability of HK-2 cells was detected by a cell counting kit-8. Data were expressed as means ± SDs (n=3). Scr changes (**C**, **D**) and ALT changes (**E**, **F**) caused by different doses of porous Se@SiO_2 nanospheres to mice were detected during 24 hours and 2 weeks. Data were expressed as means ± SDs (n=3).

Abbreviations: TEM, transmission electron microscopy; XRD, X-ray diffractometer; Scr, serum creatinine; ALT, alanine aminotransferase; ip, intraperitoneal dose.

(<5 nm) were interspersed from the center to the surface (Figure 1Ac and d).

In order to use porous Se@SiO_2 nanospheres safely and effectively, we first determined their toxicity in vivo and in vitro. As shown in Figure 1B, a concentration of 40 μg/mL was reasonable with only minimal toxicity in vitro. When the concentration exceeds 40 μg/mL, side effects could significantly inhibit cell viability and proliferation. As in our

previous research,[30] 1 mg/kg of porous Se@SiO_2 nanospheres appeared to be the appropriate dose for in vivo experiments because this concentration was associated with very little toxic damage to the liver and kidney (Figure 1C and E). We determined that this dose would not affect liver and kidney function even if administered to mice per 12 hours until 2 weeks of duration (Figure 1D and F). An excessive concentration of Se@SiO_2 would cause significant damages to both the liver and kidney, thereby elevating serum levels of alanine aminotransferase and Cr.

Se@SiO_2 reduced the production of ROS in HK-2 cells after H/R

In vitro, considerable levels of ROS were produced in HK-2 cells exposed to H/R ($P<0.05$ vs control + PBS) (Figure 2A and B). However, there was no difference in ROS production when compared between control groups with PBS or Se@SiO_2 treatment ($P>0.05$) (Figure 2A and B). Compared with the H/R + PBS group, the H/R + Se@SiO_2 group pretreated by Se@SiO_2 showed a significant reduction of ROS ($P<0.05$) (Figure 2A and B), indicating that Se@SiO_2 can suppress the hypoxia-induced production of ROS in order to protect cells against oxidative stress damage. In addition, we found that the production of GSH in the H/R groups was much lower than that in control groups, and that GSH in the H/R + Se@SiO_2 group was significantly higher than in the H/R + PBS group ($P<0.05$) (Figure 2C). GSH is the main antioxidant present in living organisms and its deficiency may result in insufficient antioxidant capacity against I/R-induced AKI. These data proved that Se@SiO_2 can not only reduce ROS levels but also preserve GSH levels in H/R.

Se@SiO_2 attenuated tubular injury and protected renal function

To determine the effect of Se@SiO_2 upon renal function in vivo, we induced renal I/R injury in experimental mice. Then, we measured levels of Cr and BUN, which are the most representative clinical indicators of renal function, at 24 hours, 72 hours, 1 week, and 2 weeks. We also evaluated renal function and found that plasma Cr and BUN levels in I/R mice were more than two times higher than those in sham mice at 24 hours ($P<0.05$) (Figure 3), which corresponded

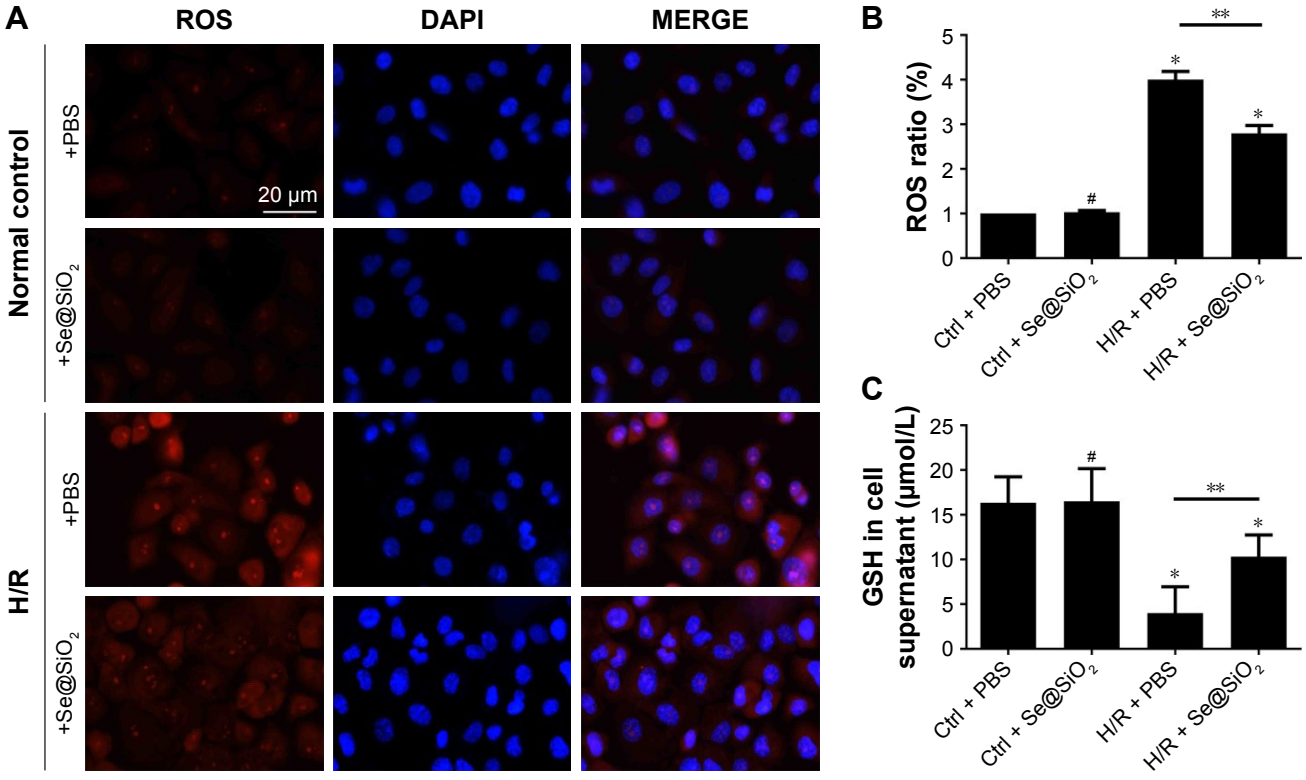

Figure 2 The level changes of ROS and GSH in HK-2 cells with different treatments.

Notes: (**A**) Staining of HK-2 cells with ROS, DAPI. Scale bars =20 μm. (**B**) Changes of ROS levels in HK-2 cells after different treatments of PBS or porous Se@SiO_2 nanospheres. Data were expressed as means ± SDs (n=10). #$P>0.05$, *$P<0.05$ vs Ctrl + PBS group, **$P<0.05$, H/R + PBS vs H/R + Se@SiO_2. (**C**) Changes of GSH levels in HK-2 cell supernatant after different treatments of PBS or porous Se@SiO_2 nanospheres. #$P>0.05$, *$P<0.05$ vs Ctrl + PBS group, **$P<0.05$, H/R + PBS vs H/R + Se@SiO_2. Data were expressed as means ± SDs (n=3).

Abbreviations: Ctrl, control; GSH, glutathione; H/R, hypoxia/reoxygenation.

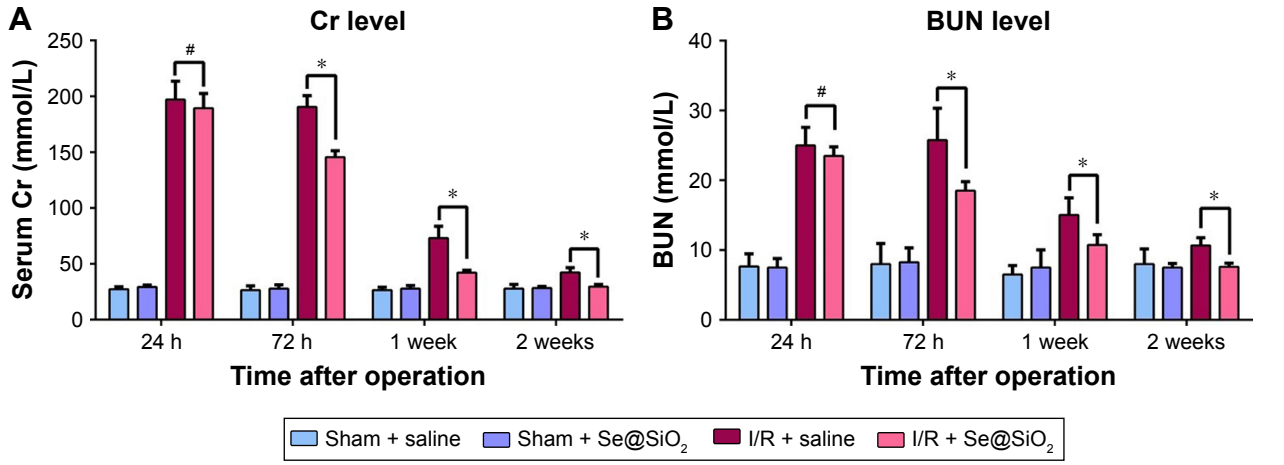

Figure 3 Cr/BUN levels in different groups of mice treated with saline or porous Se@SiO_2 nanospheres.
Notes: (**A**, **B**) There was no significant difference of Cr/BUN levels between I/R + Se@SiO_2 group and I/R + Se@SiO_2 group 24 hours after I/R. $^{\#}P>0.05$. But the levels of Cr/BUN in I/R + Se@SiO_2 group were decreased significantly compared to those in I/R + saline group from 3 days to 2 weeks after I/R. $^{*}P<0.05$. Data were expressed as means ± SDs (n≥4).
Abbreviations: Cr, creatinine; BUN, blood urea nitrogen; I/R, ischemia/reperfusion.

with the clinical diagnostic criteria for AKI.[31] Interestingly, there was no statistical difference in the levels of Cr and BUN when compared between the I/R + Se@SiO_2 group and the I/R + saline group at 24 hours ($P>0.05$). However, Se@SiO_2 treatment alone resulted in a significant reduction in Cr and BUN levels from 3 days to 2 weeks after I/R ($P<0.05$ vs I/R + saline), whereas these groups showed very little difference when tested 24 hours after I/R ($P>0.05$) (Figure 3). This indicated that Se@SiO_2 had a certain protective effect upon renal function.

Morphologically, renal TECs located in the outer medulla are extremely sensitive to intrinsic oxidative stress, particularly during the reperfusion phase.[32,33] Therefore, we further evaluated the damage caused to the outer medullary regions in each experimental group. Upon histological examination, the I/R group showed features typical of severe acute tubular damage, including extensive tubular necrosis, tubular dilatation, and loss of the brush border. Mice treated with Se@SiO_2 had significantly lower H&E scores for tubular damage after I/R ($P<0.05$ vs I/R + saline) (Figure 4A and B). Moreover, as shown in the results, the I/R + Se@SiO_2 group exhibited less cellular apoptosis ($P<0.05$ vs I/R + saline), as detected by TUNEL staining (Figure 4E and F). NGAL protein, a biomarker of AKI, is known to accumulate in the blood and urine and can be detected in patients with AKI after only a few hours.[34] We found that the proportion of NGAL-positive tissue in samples from the I/R + saline group was significantly greater than that in the I/R + Se@SiO_2 group ($P<0.05$), while the sham group was normal (Figure 4C and D). Compared to groups without Se@SiO_2 intervention, Western blotting results also showed that the expression of NGAL was inhibited in the Se@SiO_2 intervention group, both in vivo ($P<0.05$) (Figure 5C and D) and in vitro ($P<0.05$) (Figure 5A and B). Hence, these results show that intervention with Se@SiO_2 was favorable for the renal tubules and had a certain protective effect during I/R-induced AKI.

The NF-κB/NLRP3/caspase-1 pathway was suppressed by Se@SiO_2 treatment

In vivo, NF-κB, NLRP3, and caspase-1 are the main effectors of the inflammasome signaling interactive pathway, which regulates inflammatory responses. As experiments performed in vitro showed, the expression of phospho-NF-κB, NLRP3, and caspase-1 were significantly increased in the H/R groups compared with the control + PBS group ($P<0.01$) (Figure 5A and B). However, the expression of phospho-NF-κB, NLRP3, and caspase-1 in the H/R group pretreated with Se@SiO_2 were reduced significantly compared to the H/R + PBS group ($P<0.05$) (Figure 5A and B). Our in vivo experiments further showed that the increase in phospho-NF-κB, NLRP3, and caspase-1 expression in response to I/R injury was inhibited by treatment with Se@SiO_2 ($P<0.05$ vs I/R + saline group) (Figure 5C and D). Collectively, these results demonstrated that Se@SiO_2 can inhibit activation of the NF-κB/NLRP3/caspase-1 pathway.

Se@SiO_2 relieved I/R-induced inflammation both in vitro and in vivo

Next, we decided to assess whether inflammation could be reduced by Se@SiO_2 as well. Damaged TECs produce

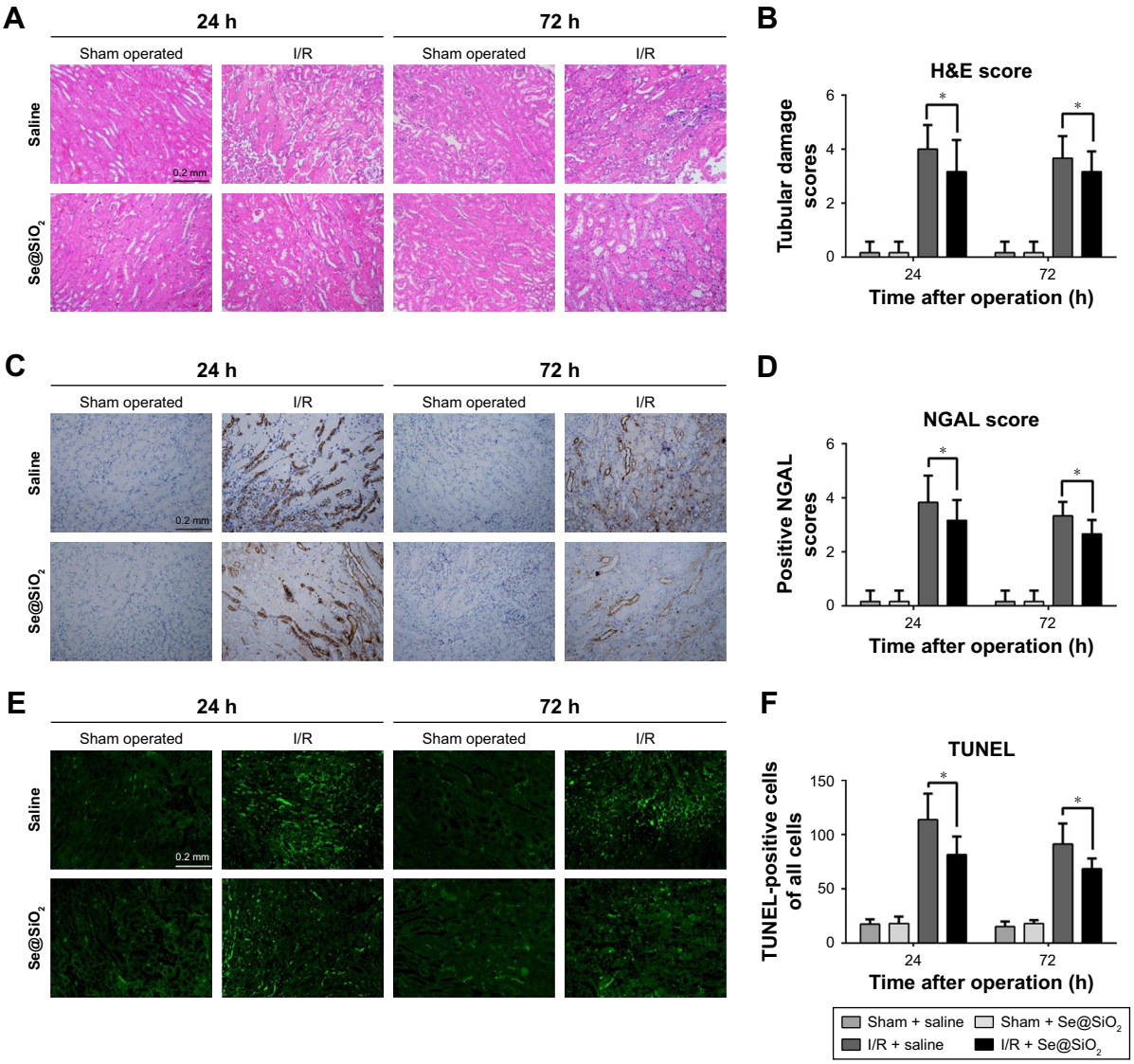

Figure 4 Histological analysis and apoptosis assessment for kidney tissues.
Notes: (**A**) Mouse kidney tissues stained with H&E. Scale bars =0.2 mm. (**B**) Tubular damage in outer medullary tissues from sham groups and I/R groups was semi-quantified using pathological scores. *$P<0.05$. Data were expressed as means ± SDs (n=10). (**C**) NGAL was detected in kidney tissues by immunohistochemistry. Scale bars =0.2 mm. (**D**) Positive NGAL area in outer medullary tissues from sham groups and I/R groups was semi-quantified using scores. *$P<0.05$. Data were expressed as means ± SDs (n=10). (**E**) Apoptosis cells in tissue were detected using a TUNEL kit. Scale bars =0.2 mm. (**F**) Statistical analysis of TUNEL staining. The numbers of TUNEL- positive cells of all cells in the field was calculated under a fluorescent microscope. *$P<0.05$. Data were expressed as means ± SDs (n=10).
Abbreviations: NGAL, neutrophil gelatinase-associated lipocalin; I/R, ischemia/reperfusion.

pro-inflammatory cytokines and chemokine, including TNF-α, IL-1β, and MCP-1, which are secreted outside of cells.[12] In vitro we found that porous Se@SiO_2 nanospheres significantly reduced pro-inflammatory cytokine production from HK-2 cells exposed to H/R ($P<0.05$ vs H/R + PBS group) (Figure 6A–C). F4/80 is a surface antigen preferentially expressed on monocytes/macrophages in mice. Macrophages are known to migrate into the outer medulla of the rat kidney following ischemia/reperfusion injury (IRI).[35] Animal models demonstrate that macrophages are a major contributor to the inflammatory response and fibrosis to AKI.[11] To assess renal inflammation after IR, we examined the number of F4/80+ cells in each group. Interestingly, with Se@SiO_2 intervention, the quantity of macrophages in kidneys exposed to I/R was significantly reduced compared to the nonintervention group, indicating that inflammatory infiltration of the kidneys was suppressed ($P<0.05$) (Figure 6D and E). These data indicate that porous Se@SiO_2 nanospheres can relieve inflammation in I/R-induced AKI.

Se@SiO_2 attenuated tubular atrophy and interstitial fibrosis

Severe ischemic AKI may progress to CKD, and is mainly characterized by renal parenchymal atrophy and interstitial

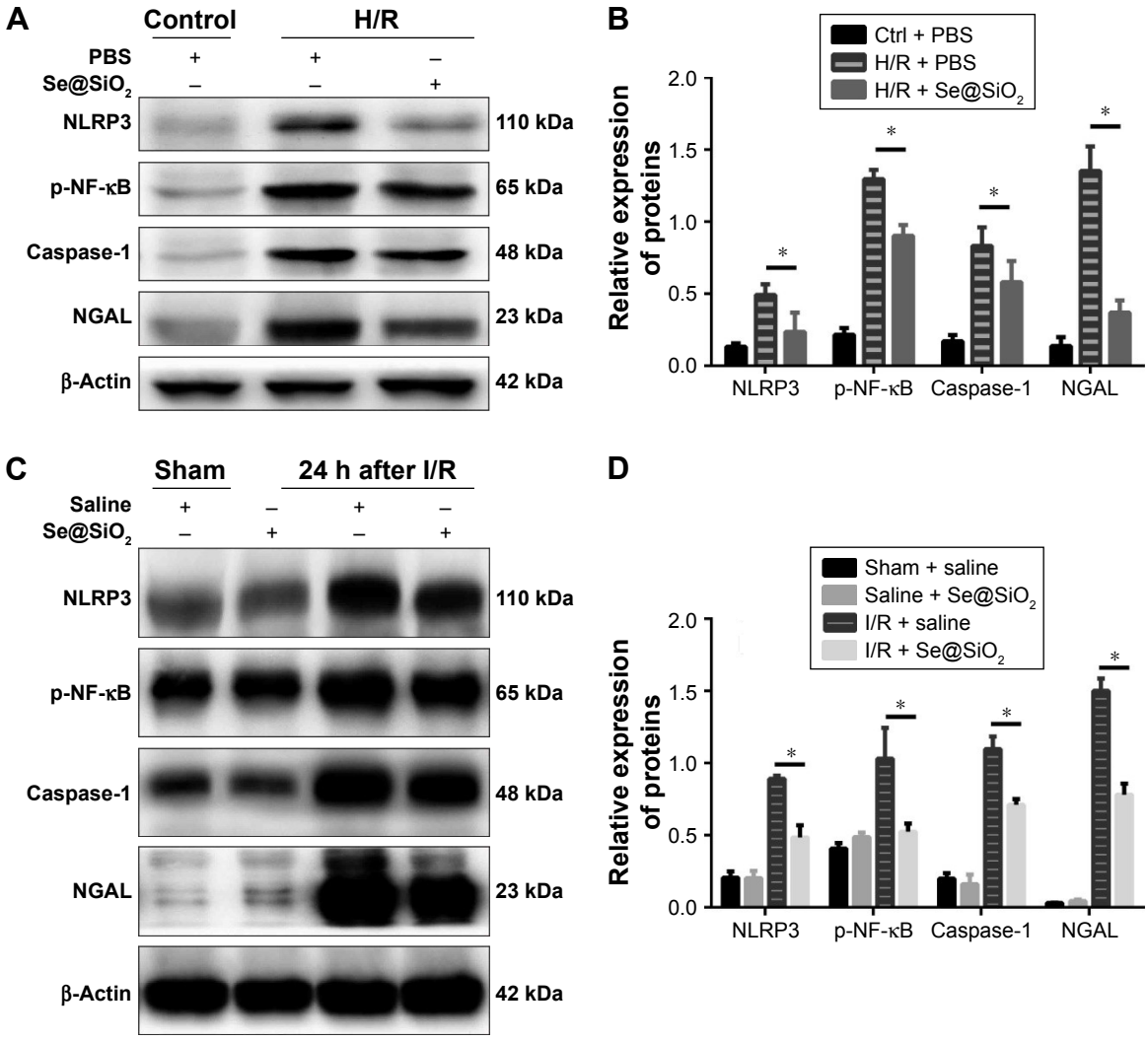

Figure 5 Expression changes of p-NF-κB/NLRP3/caspase-1 pathway and NGAL proteins with porous Se@SiO_2 nanospheres intervention in vivo and in vitro.
Notes: (**A**, **B**) Expression of p-NF-κB/NLRP3/caspase-1 and NGAL protein in HK-2 cells was determined by Western blotting. *$P<0.05$, H/R + Se@SiO_2 group vs H/R + PBS group. Data were expressed as means ± SDs (n=3). (**C**, **D**) Expression of p-NF-κB/NLRP3/caspase-1 and NGAL proteins in mouse kidney tissues was determined by Western blotting. *$P<0.05$, I/R + Se@SiO_2 group vs sham + saline group. Data were expressed as means ± SDs (n=3).
Abbreviations: p-NF-κB, phosphorylated nuclear factor-κB; NLRP3, NACHT, LRR, and PYD domains-containing protein 3; NGAL, neutrophil gelatinase-associated lipocalin; I/R, ischemia/reperfusion; H/R, hypoxia/reoxygenation.

fibrosis.[28] Renal interstitial fibrosis and tubular atrophy are the main pathological features of chronic progression after ischemic AKI.[36,37] To further investigate the effect of Se@SiO_2 on the prognosis of kidneys after AKI, we performed morphological and histological comparisons in the kidneys of mice 2 weeks after reperfusion. Masson and Sirius Red staining can specifically label collagen fibers, and can thus be used to evaluate renal fibrosis. Collagen type I, collagen type III, and α-SMA are commonly used markers used to evaluate fibrosis. Renal tubular atrophy was assessed using H&E scores (Figure 7D). Results showed that kidneys treated with Se@SiO_2 for 2 weeks after AKI exhibited less tubular atrophy and interstitial fibrosis ($P<0.05$ vs I/R + saline) (Figure 7C–G). Masson and Sirius Red staining showed appreciably increased renal fibrosis in I/R mice experiencing Se@SiO_2 treatment but a robust increase of fibrosis in I/R mice with saline treatment compared with sham groups. Renal fibrosis in I/R mice experiencing Se@SiO_2 treatment was significantly reduced compared to the I/R + saline group ($P<0.05$). Consistent with the increase in histological fibrosis, the expression of fibrotic proteins, including collagen type I, collagen type III, and α-SMA, were all increased in the I/R + Se@SiO_2 group compared with sham mice and further increased in the I/R + saline group (Figure 7A and B). In other words, early treatment with Se@SiO_2 can effectively attenuate tubular atrophy and renal fibrosis following AKI.

Discussion

AKI is a common and important diagnostic and therapeutic challenge for clinicians. Currently, it is the most frequent

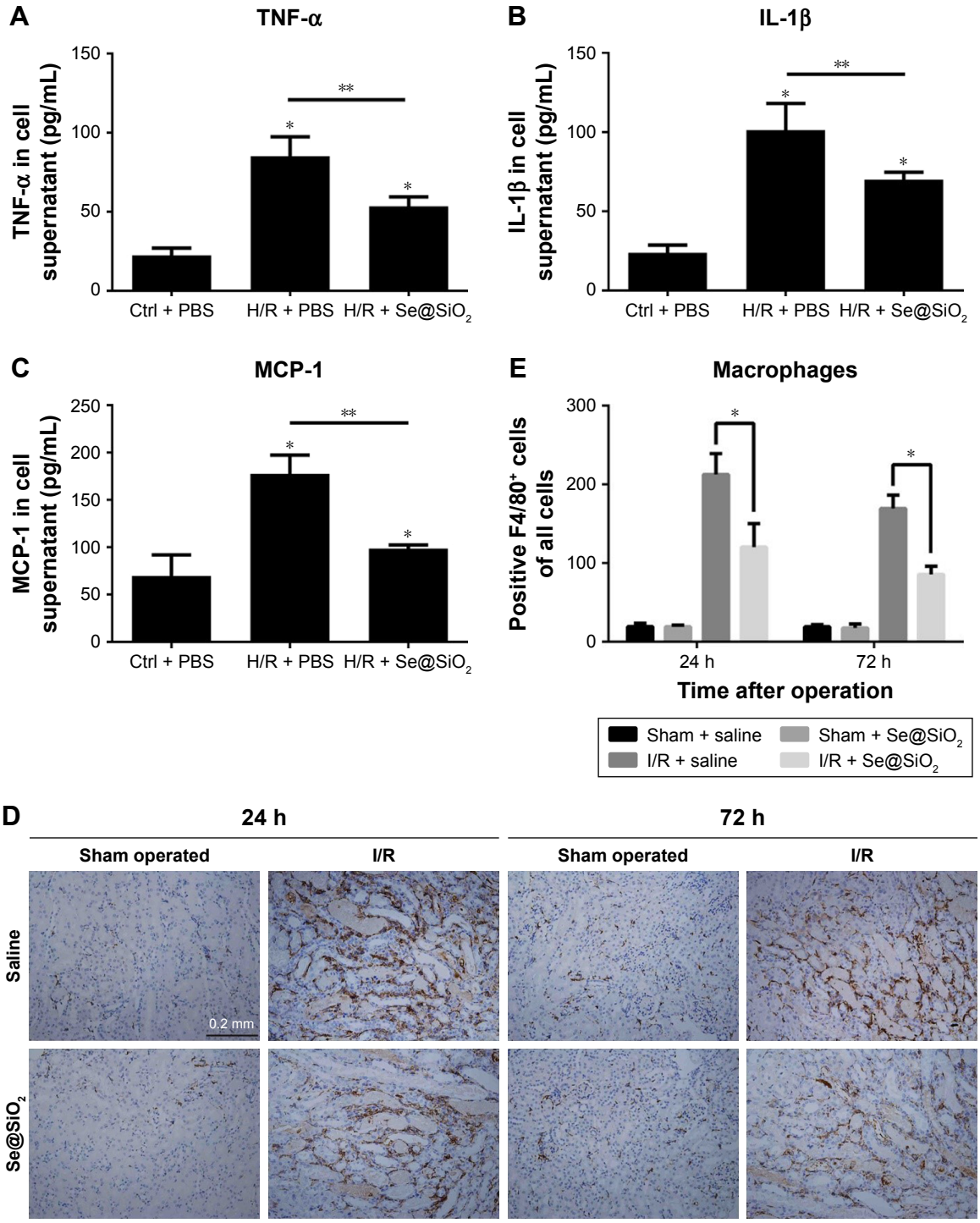

Figure 6 Changes of inflammation involving cytokines and macrophages after porous $Se@SiO_2$ nanospheres treatment.

Notes: (**A**–**C**) The secretion levels of TNF-α, IL-1β, and MCP-1 in HK-2 cells supernatant as determined by Western blotting. *$P<0.05$ vs Ctrl + PBS group, **$P<0.05$, H/R + $Se@SiO_2$ group vs H/R + PBS group. Data were expressed as means ± SDs (n=3). (**D**, **E**) Macrophage infiltration level in mouse kidney tissues was determined by immunohistochemistry for F4/80. *$P<0.05$, I/R + $Se@SiO_2$ group vs I/R + saline group. Scale bars =0.2 mm. Data were expressed as means ± SDs (n=10).

Abbreviations: TNF-α, tumor necrosis factor-α; IL-1β, interleukin-1β; MCP-1, monocyte chemotactic protein-1; Ctrl, control; I/R, ischemia/reperfusion; H/R, hypoxia/reoxygenation.

cause of organ dysfunction in ICUs and the occurrence of even mild AKI is associated with a 50% higher risk of death.[38] Furthermore, incomplete recovery from severe AKI can lead to long-term functional deficits and greater risk of progression to CKD. The kidneys of patients recovering from AKI exhibit chronic dysfunction, tubular atrophy, and interstitial fibrosis.[28] Therefore, the fundamental principle of preventing AKI is to treat the cause or trigger.[31]

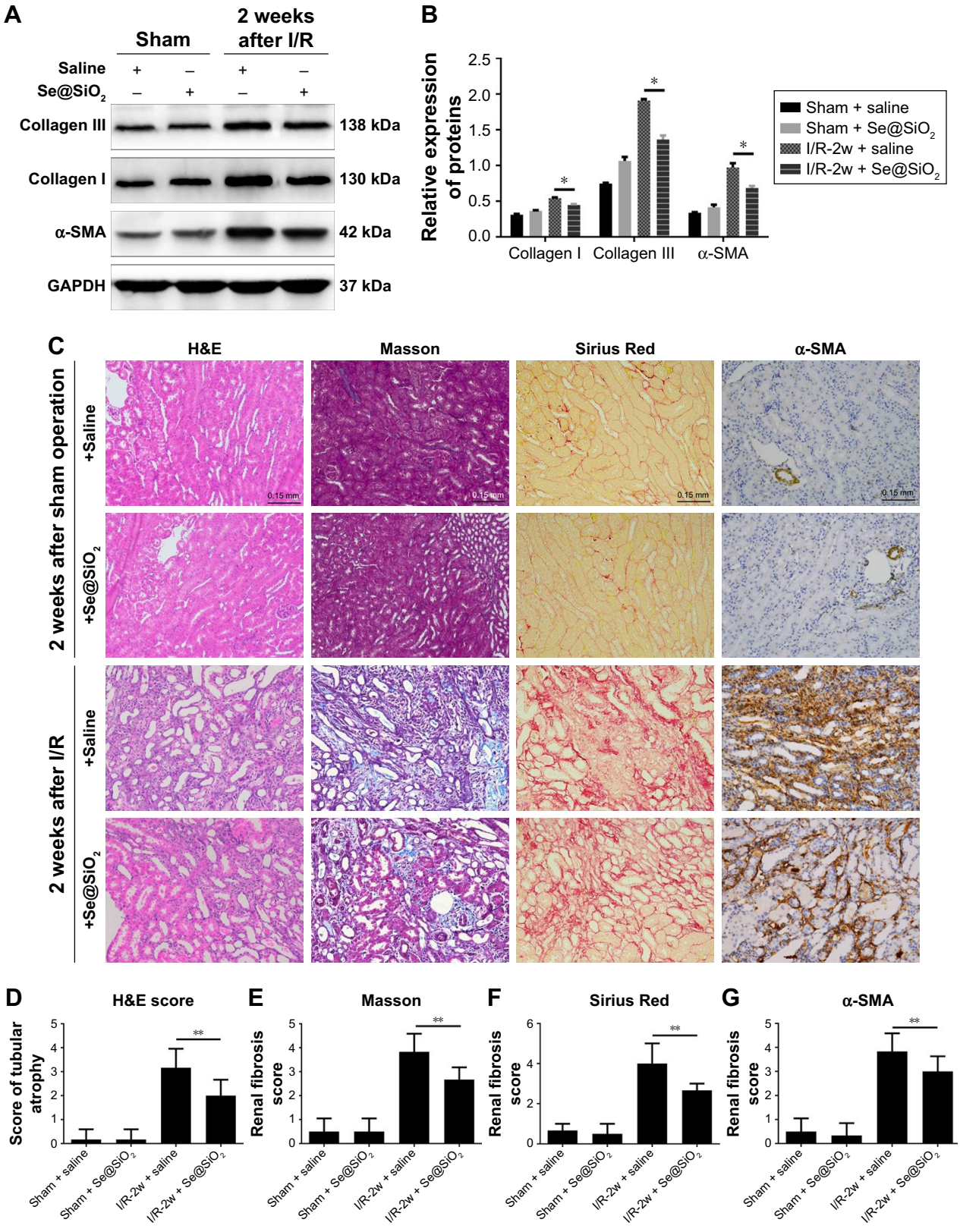

Figure 7 The effect of porous Se@SiO_2 nanospheres on renal prognosis after AKI.

Notes: (**A**, **B**) The expression levels of collagen I and III and α-SMA protein in mouse kidney tissues 2 weeks after I/R-induced AKI as detected by Western blotting. *$P<0.05$, I/R-2w + Se@SiO_2 group vs I/R-2w + saline group. Data were expressed as means ± SDs (n=3). (**C**) Renal histology H&E and fibrosis staining in 2 weeks after AKI. Scale bars =0.15 mm. Data were expressed as means ± SDs (n=10). (**D**) H&E tubule atrophy score was used to assess the severity of tubule atrophy after AKI. **$P<0.05$. Data were expressed as means ± SDs (n=10). (**E**–**G**) Masson trichrome staining, Sirius Red staining, and α-SMA immunohistochemical staining were used to assess the severity of renal fibrosis by proportion score. **$P<0.05$, I/R-2w + Se@SiO_2 group vs I/R-2w + saline group. Data were expressed as means ± SDs (n=10).

Abbreviations: α-SMA, α-smooth muscle actin; GAPDH, glyceraldehyde-3-phosphate dehydrogenase; 2w, 2 weeks; I/R, ischemia/reperfusion; AKI, acute kidney injury.

However, the mechanism underlying I/R-induced AKI is yet to be fully elucidated. Most previous studies have demonstrated that large amounts of ROS produced by H/R in I/R-induced AKI lead to TEC damage, thus activating the inflammatory signaling pathway and triggering a cascade of inflammatory responses.[8,9,39,40] TNF-α and IL-1β are regarded as important inflammatory mediators in the early stages of acute tissue injury.[41] TNF-α and IL-1β have been confirmed to regulate the activity of helper T lymphocytes, the accumulation of neutrophils, macrophages, and lymphocytes, and as mediators of the inflammatory response. MCP-1 is a small cytokine, which recruits monocytes, memory T cells, and dendritic cells to the sites of inflammation produced by either tissue injury or infection.[42,43] Ischemic AKI involves complement activation, the generation of cytokines and chemokine, including TNF-α, IL-1β, MCP-1, and infiltration of the kidney by macrophages.[12,44] Many researchers have reported that macrophages are involved in I/R-induced AKI damage and inflammation, which may stimulate fibroblasts and accelerate kidney fibrosis after AKI.[45,46]

Our current research found that proteins, including phosphorylated NF-κB (p-NF-κB), NLRP3, and caspase-1, were highly expressed in kidney tissue experiencing IRI. It was previously reported that NF-κB and NLRP3 are involved in AKI.[16–18,47,48] NF-κB regulates the expression of numerous genes, including cytokines/chemokines, cell adhesion molecules, and stress response genes. p-NF-κB is trafficked into the nucleus to activate the expression of inflammatory cytokines (IL-1β, TNF-α, IL-6, etc) and then forms an "inflammatory cascade" to initiate renal interstitial inflammation.[49] NLRP3−/− mice are protected against ischemic AKI, thus confirming that the role of the NLRP3 inflammasome is unfavorable in ischemic AKI.[17,18] Interestingly, our results showed that increased levels of cytokines (TNF-α, IL-1β, MCP-1) and proteins (p-NF-κB, NLRP3, caspase-1) were not significant owing to the intervention of porous Se@SiO_2 nanospheres. Thus, these results indicated that porous Se@SiO_2 nanospheres may alleviate I/R-induced inflammation by resisting ROS.

In terms of the long-term outcome after AKI, more and more studies have found that ischemic AKI is associated with tubular interstitial inflammation, which may contribute to renal atrophy and sclerosis in the future.[37,50] The combination of tubular atrophy and tubular interstitial fibrosis (TIF) is an important hallmark of CKD because tubular atrophy has repeatedly been shown to be superior to glomerular pathology as a predictor of CKD progression.[51,52] Based on existing research and data, we can hypothesize that the kidney develops a strong oxidative stress response while experiencing I/R injury. Subsequently, there is a long-term inflammatory reaction in the kidney which includes the infiltration of monocytes and lymphocytes, which contribute to the proliferation of renal interstitial fibroblasts. Renal tubules exposed to severe injury gradually undergo atrophy, which makes the structure of the kidney change irreversibly, thus leading to abnormal functionality. The outcome of TIF and tubular atrophy appears to be responsible for the progression from AKI to CKD (Figure 8). Reducing the prevalence of CKD is therefore of utmost importance. Therefore, reducing the severity of injury in early AKI, attenuating oxidative stress, and restricting or preventing further enhanced inflammatory responses are the key to preventing AKI–CKD transformation (Figure 8).

As a trace element, Se exerts strong antioxidant properties and participates in regulating the activity of GSH.[53] However, Se also has cytotoxic properties, and a relatively narrow dose range separates physiological effects from toxicity.[54] The porous structure of Se@SiO_2 nanospheres means that they are slow-releasing and provide favorable biocompatibility. In vitro, intervention with porous Se@SiO_2 nanospheres could significantly reduce the levels of ROS (Figure 2A and B) and inflammatory cytokines (TNF-α, IL-1β, MCP-1) (Figure 6A–C) produced by HK-2 cells after H/R treatment. In vivo, porous Se@SiO_2 nanospheres significantly attenuated renal tubular damage (Figure 4A–D) and reduced cell apoptosis (Figure 4E and F) and macrophage infiltration (Figure 6D and E) during AKI. Moreover, the occurrence of fibrosis and tubular atrophy after AKI was reduced significantly following the injection of porous Se@SiO_2 nanospheres (Figure 7). Results showed that porous Se@SiO_2 nanospheres effectively inhibited the increased expression of phospho-NF-κB, NLRP3, and caspase-1 when AKI occurred in vivo and in vitro (Figure 5A–D). However, the specific mechanism underlying how the porous Se@SiO_2 nanospheres can inhibit the inflammatory signaling pathway effector molecules p-NF-κB, NLRP3, and caspase-1, and whether the anti-inflammatory effect of Se@SiO_2 occurs directly through the inhibition of the inflammatory pathway or indirectly by combatting oxidative stress remain unclear and require further investigation.

In addition, whether Se@SiO_2 can play the same role in human beings is still uncertain. Moreover, the optimal administration method and administration time for porous Se@SiO_2 nanospheres for I/R-induced AKI have still to be defined. It is therefore important that future work addresses the specific therapeutic mechanisms of Se@SiO_2.

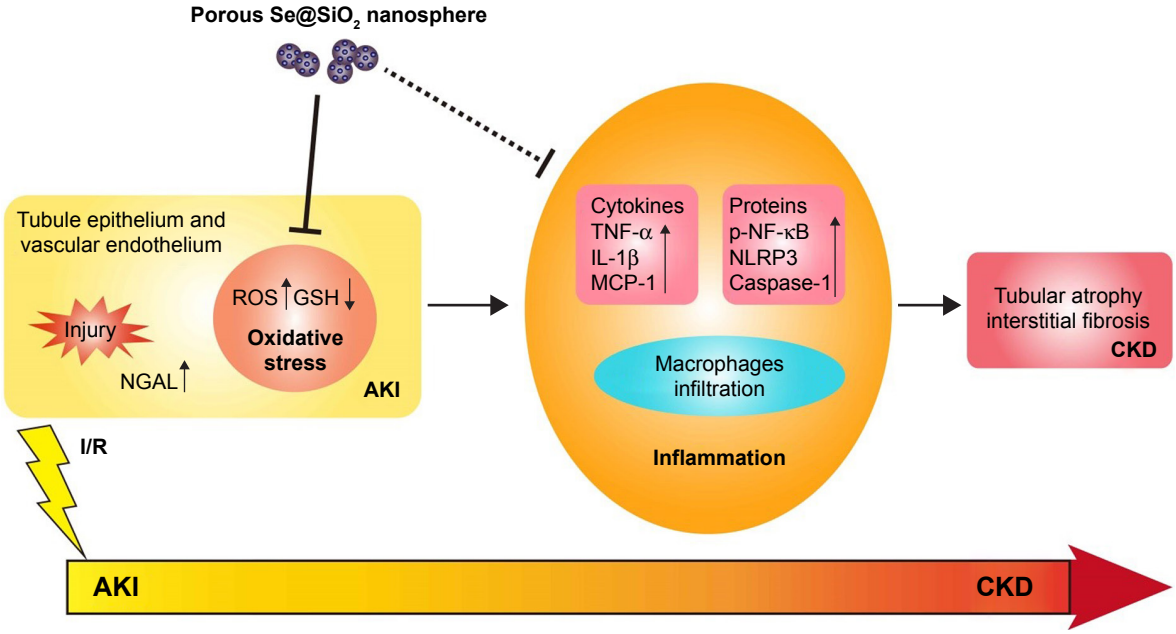

Figure 8 The description of porous Se@SiO$_2$ nanospheres attenuating ischemic AKI injury and improving prognosis.
Note: Porous Se@SiO$_2$ nanospheres attenuate ischemic AKI injury and improve prognosis by reducing the severity of injury in early AKI, resisting oxidative stress, relieving inflammation, and preventing further transition of AKI to CKD.
Abbreviations: AKI, acute kidney injury; GSH, glutathione; CKD, chronic kidney disease; TNF-α, tumor necrosis factor-α; IL-1β, interleukin-1β; MCP-1, monocyte chemotactic protein-1; p-NF-κB, phosphorylated nuclear factor-κB; NLRP3, NACHT, LRR, and PYD domains-containing protein 3; NGAL, neutrophil gelatinase-associated lipocalin.

Conclusion

In this study, we verified that Se@SiO$_2$ reduced the production of ROS, preserved GSH, and diminished the expression of inflammation-associated proteins and cytokines. Consequently, Se@SiO$_2$ could alleviate oxidative stress and inflammation, exhibiting a protective effect for the kidney in AKI. Subsequently, tubular atrophy and fibrosis were attenuated by Se@SiO$_2$ intervention. Hence, porous Se@SiO$_2$ nanospheres were effective agents which may represent a new therapeutic method for the clinical therapy of AKI and prevent the transition from AKI to CKD.

Acknowledgments

This work was supported by the National Natural Science Foundation of China (grant no 21476136), Natural Science Foundation of Shanghai (grant no 15ZR1433500), Science and Technology Commission of Shanghai Municipality (grant no 15140902900), China and medical-engineering funding of Shanghai Jiao Tong University (grant no ZH2018QNA20).

Author contributions

ZZheng, GD, CQ, YX and ZZhao performed the studies and statistical analyses, interpreted the data, and wrote the manuscript. XL and YC collected the materials and managed references. ZZhang, HW, and JL conducted the experiments. ZZheng, GD, CQ, YX, YC, ZZhang, HW and JL have revised the manuscript critically and prepared the final version of the manuscript. All authors contributed to data analysis, drafting and revising the article, gave final approval of the version to be published, and agree to be accountable for all aspects of the work.

Disclosure

The authors report no conflicts of interest in this work.

References

1. Chawla LS, Bellomo R, Bihorac A, et al. Acute kidney disease and renal recovery: consensus report of the Acute Disease Quality Initiative (ADQI) 16 Workgroup. *Nat Rev Nephrol*. 2017;13(4):241–257.
2. Hoste EA, Bagshaw SM, Bellomo R, et al. Epidemiology of acute kidney injury in critically ill patients: the multinational AKI-EPI study. *Intensive Care Med*. 2015;41(8):1411–1423.
3. Lewington AJ, Cerdá J, Mehta RL. Raising awareness of acute kidney injury: a global perspective of a silent killer. *Kidney Int*. 2013;84(3):457–467.
4. Hsu CY. Yes, AKI truly leads to CKD. *J Am Soc Nephrol*. 2012;23(6):967–969.
5. Waikar SS, Winkelmayer WC. Chronic on acute renal failure: long-term implications of severe acute kidney injury. *JAMA*. 2009;302(11):1227–1229.
6. Kam Tao Li P, Burdmann EA, Mehta RL, World Kidney Day Steering Committee 2013. Acute kidney injury: Global health alert. *J Nephropathol*. 2013;2(2):90–97.
7. Zhang YL, Qiao SK, Wang RY, Guo XN. NGAL attenuates renal ischemia/reperfusion injury through autophagy activation and apoptosis inhibition in rats. *Chem Biol Interact*. 2018;289:40–46.

8. Winterberg PD, Wang Y, Lin KM, et al. Reactive oxygen species and IRF1 stimulate IFNα production by proximal tubules during ischemic AKI. *Am J Physiol Renal Physiol*. 2013;305(2):F164–F172.
9. Gu Y, Huang F, Wang Y, et al. Connexin 32 plays a crucial role in ROS-mediated endoplasmic reticulum stress apoptosis signaling pathway in ischemia reperfusion-induced acute kidney injury. *J Transl Med*. 2018;16(1):117.
10. Andres-Hernando A, Li N, Cicerchi C, et al. Protective role of fructokinase blockade in the pathogenesis of acute kidney injury in mice. *Nat Commun*. 2017;8:14181.
11. Huen SC, Cantley LG. Macrophages in Renal Injury and Repair. *Annu Rev Physiol*. 2017;79(1):449–469.
12. Rabb H, Griffin MD, Mckay DB, et al. Inflammation in AKI: Current Understanding, Key Questions, and Knowledge Gaps. *J Am Soc Nephrol*. 2016;27(2):371–379.
13. Friedewald JJ, Rabb H. Inflammatory cells in ischemic acute renal failure. *Kidney Int*. 2004;66(2):486–491.
14. Mulay SR, Linkermann A, Anders HJ. Necroinflammation in Kidney Disease. *J Am Soc Nephrol*. 2016;27(1):27–39.
15. Devarajan P. Update on mechanisms of ischemic acute kidney injury. *J Am Soc Nephrol*. 2006;17(6):1503–1520.
16. Szeto HH, Liu S, Soong Y, et al. Mitochondria Protection after Acute Ischemia Prevents Prolonged Upregulation of IL-1β and IL-18 and Arrests CKD. *J Am Soc Nephrol*. 2017;28(5):1437–1449.
17. Kim HJ, Lee DW, Ravichandran K, et al. NLRP3 inflammasome knockout mice are protected against ischemic but not cisplatin-induced acute kidney injury. *J Pharmacol Exp Ther*. 2013;346(3):465–472.
18. Markó L, Vigolo E, Hinze C, et al. Tubular Epithelial NF-κB Activity Regulates Ischemic AKI. *J Am Soc Nephrol*. 2016;27(9):2658–2669.
19. Ebert R, Ulmer M, Zeck S, et al. Selenium supplementation restores the antioxidative capacity and prevents cell damage in bone marrow stromal cells in vitro. *Stem Cells*. 2006;24(5):1226–1235.
20. Deng G, Chen C, Zhang J. Se@SiO_2 nanocomposites attenuate doxorubicin-induced cardiotoxicity through combatting oxidative damage. *Artif Cells Nanomed Biotechnol*. 2018;150:1–10.
21. Deng G, Dai C, Chen J, et al. Porous Se@SiO_2 nanocomposites protect the femoral head from methylprednisolone-induced osteonecrosis. *Int J Nanomedicine*. 2018;13:1809–1818.
22. Zhu Y, Deng G, Ji A, et al. Porous Se@SiO_2 nanospheres treated paraquat-induced acute lung injury by resisting oxidative stress. *Int J Nanomedicine*. 2017;12:7143–7152.
23. Liu X, Deng G, Wang Y, et al. A novel and facile synthesis of porous SiO2-coated ultrasmall Se particles as a drug delivery nanoplatform for efficient synergistic treatment of cancer cells. *Nanoscale*. 2016;8(16):8536–8541.
24. Wu CC, Chang CY, Chang ST, Chen SH. 17β-Estradiol Accelerated Renal Tubule Regeneration in Male Rats After Ischemia/Reperfusion-Induced Acute Kidney Injury. *Shock*. 2016;46(2):158–163.
25. Tanaka R, Yazawa M, Morikawa Y, et al. Sex differences in ischaemia/reperfusion-induced acute kidney injury depends on the degradation of noradrenaline by monoamine oxidase. *Clin Exp Pharmacol Physiol*. 2017;44(3):371–377.
26. Kang KP, Lee JE, Lee AS, Lee AESIN, et al. Effect of gender differences on the regulation of renal ischemia-reperfusion-induced inflammation in mice. *Mol Med Rep*. 2014;9(6):2061–2068.
27. Ikeda M, Swide T, Vayl A, Lahm T, Anderson S, Hutchens MP. Estrogen administered after cardiac arrest and cardiopulmonary resuscitation ameliorates acute kidney injury in a sex- and age-specific manner. *Crit Care*. 2015;19(1):332.
28. Venkatachalam MA, Weinberg JM, Kriz W, Bidani AK. Failed Tubule Recovery, AKI-CKD Transition, and Kidney Disease Progression. *J Am Soc Nephrol*. 2015;26(8):1765–1776.
29. Zhang D, Liu Y, Wei Q, et al. Tubular p53 regulates multiple genes to mediate AKI. *J Am Soc Nephrol*. 2014;25(10):2278–2289.
30. Deng G, Niu K, Zhou F, et al. Treatment of steroid-induced osteonecrosis of the femoral head using porous Se@SiO_2 nanocomposites to suppress reactive oxygen species. *Sci Rep*. 2017;7(1):43914.
31. Bellomo R, Kellum JA, Ronco C. Acute kidney injury. *Lancet*. 2012;380(9843):756–766.
32. Brezis M, Rosen S. Hypoxia of the renal medulla – its implications for disease. *N Engl J Med*. 1995;332(10):647–655.
33. Jiang M, Wei Q, Dong G, Komatsu M, Su Y, Dong Z. Autophagy in proximal tubules protects against acute kidney injury. *Kidney Int*. 2012;82(12):1271–1283.
34. Bennett M, Dent CL, Ma Q, et al. Urine NGAL predicts severity of acute kidney injury after cardiac surgery: a prospective study. *Clin J Am Soc Nephrol*. 2008;3(3):665–673.
35. Ysebaert DK, de Greef KE, Vercauteren SR, et al. Identification and kinetics of leukocytes after severe ischaemia/reperfusion renal injury. *Nephrol Dial Transplant*. 2000;15(10):1562–1574.
36. Wang W, Wang A, Luo G, Ma F, Wei X, Bi Y. S1P1 receptor inhibits kidney epithelial mesenchymal transition triggered by ischemia/reperfusion injury via the PI3K/Akt pathway. *Acta Biochim Biophys Sin*. 2018;50(7):651–657.
37. Liu Y. Epithelial to mesenchymal transition in renal fibrogenesis: pathologic significance, molecular mechanism, and therapeutic intervention. *J Am Soc Nephrol*. 2004;15(1):1–12.
38. Linder A, Fjell C, Levin A, Walley KR, Russell JA, Boyd JH. Small acute increases in serum creatinine are associated with decreased long-term survival in the critically ill. *Am J Respir Crit Care Med*. 2014;189(9):1075–1081.
39. Liu L, Wu X, Xu H. Myocardin-related transcription factor A (MRTF-A) contributes to acute kidney injury by regulating macrophage ROS production. *Biochim Biophys Acta*. 2018;1864(10):3109–3121.
40. Meng XM, Ren GL, Gao L, et al. NADPH oxidase 4 promotes cisplatin-induced acute kidney injury via ROS-mediated programmed cell death and inflammation. *Lab Invest*. 2018;98(1):63–78.
41. Prieto-Moure B, Lloris-Carsí JM, Belda-Antolí M, Toledo-Pereyra LH, Cejalvo-Lapeña D. Allopurinol Protective Effect of Renal Ischemia by Downregulating TNF-α, IL-1β, and IL-6 Response. *J Invest Surg*. 2017;30(3):143–151.
42. Gura T. Immunology: Chemokines Take Center Stage in Inflammatory Ills. *Science*. 1996;272(5264):954–956.
43. Carr MW, Roth SJ, Luther E, Rose SS, Springer TA. Monocyte chemoattractant protein 1 acts as a T-lymphocyte chemoattractant. *Proc Natl Acad Sci U S A*. 1994;91(9):3652–3656.
44. Thurman JM. Triggers of inflammation after renal ischemia/reperfusion. *Clin Immunol*. 2007;123(1):7–13.
45. Lee S, Huen S, Nishio H, et al. Distinct macrophage phenotypes contribute to kidney injury and repair. *J Am Soc Nephrol*. 2011;22(2):317–326.
46. Cao Q, Harris DC, Wang Y. Macrophages in kidney injury, inflammation, and fibrosis. *Physiology*. 2015;30(3):183–194.
47. Hu L, Chen C, Zhang J, et al. IL-35 Pretreatment Alleviates Lipopolysaccharide-Induced Acute Kidney Injury in Mice by Inhibiting NF-κB Activation. *Inflammation*. 2017;40(4):1393–1400.
48. Wen Y, Liu YR, Tang TT, et al. mROS-TXNIP axis activates NLRP3 inflammasome to mediate renal injury during ischemic AKI. *Int J Biochem Cell Biol*. 2018;98:43–53.
49. Aksentijevich I, Zhou Q. NF-κB Pathway in Autoinflammatory Diseases: Dysregulation of Protein Modifications by Ubiquitin Defines a New Category of Autoinflammatory Diseases. *Front Immunol*. 2017;8:399.
50. Zeisberg M, Neilson EG. Mechanisms of tubulointerstitial fibrosis. *J Am Soc Nephrol*. 2010;21(11):1819–1834.
51. Rosenbaum JL, Mikail M, Wiedmann F. Further correlation of renal function with kidney biopsy in chronic renal disease. *Am J Med Sci*. 1967;254(2):156–160.
52. Bohle A, Mackensen-Haen S, von Gise H. Significance of tubulointerstitial changes in the renal cortex for the excretory function and concentration ability of the kidney: a morphometric contribution. *Am J Nephrol*. 1987;7(6):421–433.
53. Birringer M, Pilawa S, Flohé L. Trends in selenium biochemistry. *Nat Prod Rep*. 2002;19(6):693–718.
54. Wang Y, Chen P, Zhao G, et al. Inverse relationship between elemental selenium nanoparticle size and inhibition of cancer cell growth in vitro and in vivo. *Food Chem Toxicol*. 2015;85:71–77.